Low-Dimensional Forest-Like and Desert-Like Fractal Patterns Formed in a DDAN Molecular System *

CAI Jin-Ming(蔡金明)[1], BAO Li-Hong(鲍丽宏)[1], GUO Wei(郭伟)[1], CAI Li(蔡莉)[1], HUAN Qing(郇庆)[1], LIAN Ji-Chun(连季春)[1], GUO Hai-Ming(郭海鸣)[1], WANG Ke-Zhi(王科志)[2], SHI Dong-Xia(时东霞)[1], PANG Shi-Jin(庞世谨)[1], GAO Hong-Jun(高鸿钧)[1**]

[1]*Beijing National Laboratory of Condensed Matter Physics and Institute of Physics, Chinese Academy of Sciences, Beijing 100080*

[2]*Department of Chemistry, Beijing Normal University, Beijing 100871*

(Received 29 January 2007)

Two kinds of forest-like and desert-like patterns are formed by thermal evaporation of 4-dicyanovinyl-N, N-dimethylamino-1-naphthalene (DDAN) onto SiO_2 substrates. Based on thermal kinetics of the molecules on the substrate the transformation between the forest and desert patterns is due to two factors. The first one is the diffusion length, which is related to the deposition rate, the diffusion potential energy barrier and the substrate temperature. The second one is the strong interaction between the two polarity chemical groups of the molecules, which is beneficial to the formation of branches. Totally different patterns are also found on mica substrates, and are attributed to the anisotropic diffusion and the stronger interaction between DDAN molecules and the mica surface.

PACS: 68.55.Ac, 68.65.−k, 64.60.Ak

Over the last few decades, fractal organic thin films have attracted a great interest in fields of physics and mathematics.[1−7] The fractal growth patterns show a variety of related problems, such as the electrodeposition, dielectric breakdown, viscous fingering, crystal growth, and the amorphous structural transformation.[8,9] Thus it is important to understand the formation mechanism of the fractional structures in experiments and theories.[10−21] On the other hand, a new class of organic molecules named charge transfer complex (CTC), which usually are conjugate systems, has emerged as a new focus in the past few years because of their many exciting optic, electronic and photoelectric properties.[22−25]

The molecule 4-dicyanovinyl-N, N-dimethylamino-1- naphthalene (DDAN) was chosen because it represents a typical CTC molecule with novel structure and photoelectric properties.[26−30] The DDAN molecular structure is shown in Fig. 1. It is a planar molecule of conjugate structure, in which a naphthalene in the middle, two cyano-groups of one side, and a dimethyl amino group of the other side. Based on the structural properties, special patterns may be attained as a result of the planar structure and the intermolecular attraction between the electron donor, -N(CH_3)$_2$, and the electron acceptor, -CN.[31−33] Otherwise, based on a previous work of pentacene film growth, Malliaras concluded that there are three main growth parameters, which play an important role in the growth process, as follows: (1) nature of the substrate, (2) substrate temperature and deposition rate, (3) kinetic energy of the molecular beam.[34] We can conduct our research on the growth properties of DDAN thin films using the similar methods.

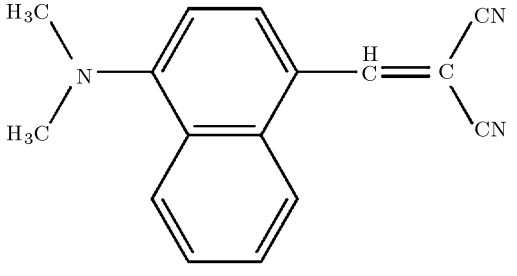

Fig. 1. Chemical structure of 4-dicyanovinyl-N, N-dimethylamino-1-naphthalene (DDAN). It is a conjugate system with an electron donor -N(CH_3)$_2$ and an electron acceptor -CN.

In this Letter, we present the growth of DDAN thin films by adjusting the evaporation temperature and time, substrate temperature, and the amount of evaporating molecules. Meanwhile, both amorphous SiO_2 and mica substrates are used to compare the influence of the interaction between the molecules and the substrate in the film growth. A systematic investigation on the initial adsorption of the DDAN thin films is carried out and the formation mechanism of different patterns is discussed based on thermal kinetics of the molecules on the substrate. Two main patterns, 'forest-like' and 'desert-like', are formed on SiO_2 substrates. The transformation between these two patterns can be controlled by adjusting the growth conditions. These results can be a guidance for formation of DDAN thin films with desired patterns and other ordered organic CTC thin films.

A home-made physical vapour deposition system is

* Supported by the National Natural Science Foundation of China under Grant No 90406022. the Hi-Tech Research and Development Programme of China under Grant No 2004AA302G11, and the National Basic Research Programme of China under Grant No 2006CB921305.

** Email: hjgao@aphy.iphy.ac.cn

used to grow the DDAN films. The background pressure in the chamber is better than 1.0×10^{-5} Torr. We vary the evaporation temperature and time, the substrate temperature, the amount of the evaporation molecules, and the substrate type to explore the formation mechanism of the growth patterns as well as their transformation. During this process, only one parameter is varied while keeping others fixed in order to single out the effect. For comparison, amorphous SiO_2 and crystalline mica are used as the substrates. The morphologies of different patterns are observed using an atomic forced microscope (AFM, Multimode^{TM} SPM, Digital Instrument Company).

Two kinds of patterns are observed on the SiO_2 substrates. One is of some dendritic crystal interlaced with each other, similar to the treetop of a forest. The other is of small sized particles aggregating together as in a desert. Thus we name the two patterns as the forest and desert patterns which are two different objects in nature. Figure 2 shows the AFM images of these patterns grown at different evaporation temperatures of 70°C to 100°C on the SiO_2 substrate. The forest pattern is obtained at low evaporation temperature while the desert pattern is obtained at high evaporation temperature. Perfect dendritic branches are formed at 70°C with a length of about $4\,\mu$m and a width of about 600 nm (Fig. 2(a)). Both particles and branches are achieved at 80°C, 90°C and 100°C as shown in Figs. 2(b), 2(c) and 2(d), respectively. There is a trend that particles aggregate into branches in Fig. 2(b). Figures 2(c) and 2(d) show that a few shorter branches are formed and are surrounded by particles with a diameter of about $1\,\mu$m close to the width of the central branches. Additionally, the pattern at 100°C in Fig. 2(d) has a larger particle density than that at 90°C in Fig. 2(c), and branches in Fig. 2(d) centre can hardly be seen. The above observation shows that the forest pattern is gradually evolving into the desert pattern with the increasing temperature.

Here we try to apply diffusion theory to understand the influence of evaporation temperature on different pattern formations. It is well known that the resident time and the diffusion length of the molecules play an important role in the nucleation and growth. The resident time τ_a is related to the adsorptive energy E_a by constant, T is the substrate temperature, and f is the vibration frequency in the vertical direction. We take v to represent the diffusion steps in unit interval and it is related to the diffusion activation energy E_d by $v = f_1 \exp(E_d/k_bT)$, where f_1 is the vibration frequency in the transverse direction. We consider that $f_1 \sim f$ because of the same magnitude. Thus we could derive the total diffusion steps during the resident time,

$$m = v\tau_a = \exp[(E_a - E_d)/k_bT]. \tag{1}$$

Regarding to the amorphous SiO_2 substrate, the interaction between the molecule and the substrate is quite weak.[34] Thus the adsorptive energy E_a is much smaller than the diffusion activation energy E_d and thus can be neglected. We have

$$m = \exp[-E_d/k_bT]. \tag{2}$$

If the total diffusion steps m is divided by the number of deposited molecules, we can obtain the steps each molecule diffuses on the substrate,

$$\lambda \propto R^{-1} \exp[-E_d/k_bT], \tag{3}$$

where λ is the diffusion length determined by the diffusion steps, and R is the deposition rate. According to this equation, we know how far the molecules diffuse on the substrate as a function of the substrate temperature T and the deposition rate R.

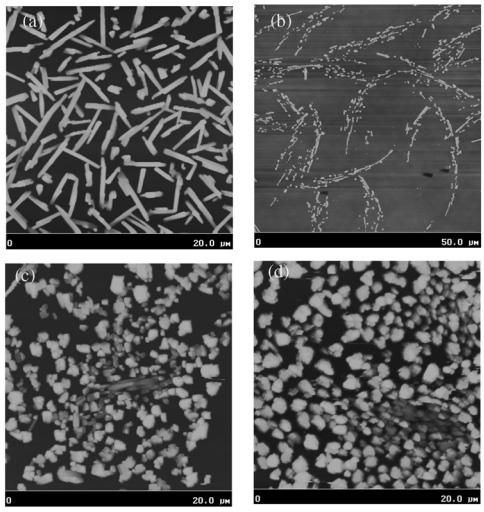

Fig. 2. AFM images of organic patterns prepared at different evaporation temperatures from 70°C to 100°C on SiO_2 substrates. (a) Evaporation at 70°C for 2 min, $P = 3.6 \times 10^{-5}$ Torr. (b) Evaporation at 80°C for 2 min, $P = 2.2 \times 10^{-6}$ Torr. (c) Evaporation at 90°C for 2 min, $P = 4.0 \times 10^{-6}$ Torr. (d) Evaporation at 100°C for 2 min, $P = 3.6 \times 10^{-5}$ Torr. The forest pattern is obtained at low evaporation temperature while the desert pattern is obtained at high evaporation temperature. The forest pattern is changing gradually into the desert pattern with the increasing temperature.

A change of the evaporation temperature will affect the beam current which in turn determines the deposition rate. Obviously, the higher the evaporation temperature, the higher the evaporation rate. A DDAN molecule could diffuse a longer distance at a lower deposition rate than that at a higher deposition rate according to Eq. (3). Meanwhile, the DDAN molecule is a conjugate system which has both the electron donor -$N(CH_3)_2$ and the electron acceptor -CN, thus the two polarity groups should have a much strong interaction to aggregate hand by hand to form branches along the interaction direction. Additionally, the SiO_2 substrate is isotropic and the interaction between the molecules and the substrate is weak.[34] Under this condition, the DDAN molecules should diffuse freely for a long time with rare collisions at the low evaporation temperature to form dendritic branches.

On the other hand, the DDAN molecules at high evaporation temperature could not diffuse for a long distance thus should form short branches and particles instead.

We also investigate the relationship between different pattern formations and the evaporation time. Figure 3 shows the AFM images of different patterns at different evaporation times at 90°C. About 40-μm-long branches attached by some little particles with a diameter of about 1 μm are formed for 1 min evaporation time (Fig. 3(a)). The pattern shows many particles surrounding the central branches as the evaporation time reaches 3 min (Fig. 3(b)), and the nearly 8-μm-long branches become much shorter than those grown for 1 min. For 5 min evaporation time, the pattern (Fig. 3(c)) consists of much larger particles of about 2 μm diameter and fewer central branches. These results indicate that the forest pattern evolves into the desert pattern with the increasing evaporation time.

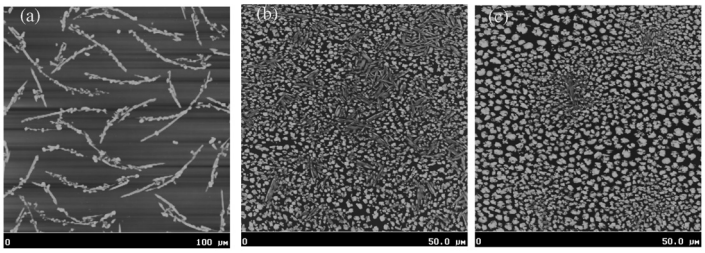

Fig. 3. AFM images of patterns synthesized at different evaporation times on SiO_2 substrates. (a) Evaporation at 90°C for 1 min, $P = 2.2 \times 10^{-6}$ Torr. (b) Evaporation at 90°C for 3 min, $P = 8.0 * 10^{-6}$ Torr. (c) Evaporation at 90°C for 5 min, $P = 1.0 * 10^{-5}$ Torr. Long branches are formed for 1 min evaporating time. Molecules can no longer reach the branch top to form long branches. Instead, the molecules form short branches with particles attaching to the side of long branches. The forest pattern changes into the desert pattern with the increasing evaporation time.

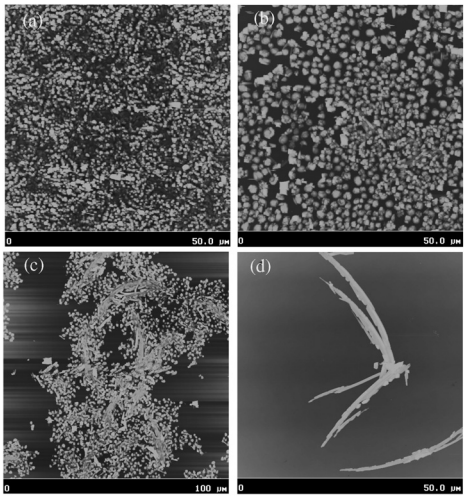

Fig. 4. AFM images of the organic patterns evaporated for 10 min at 90°C on SiO_2 surface, when the substrate temperature varied from 25°C to 40°C. (a) Substrate temperature 25°C, $P = 3.2 \times 10^{-6}$ Torr. (b) Substrate temperature 30°C, $P = 2.4 \times 10^{-6}$ Torr. (c) Substrate temperature 35°C, $P = 2.2 \times 10{-}6$ Torr. (d) Substrate temperature 40°C, $P = 4.0 \times 10^{-6}$ Torr. Molecules can form long branches at high substrate temperature because the diffusion distance λ of the DDAN molecules become longer at high substrate temperature T. Thus the desert-to-forest pattern transformation is a result of increasing the diffusion distance.

We know that the evaporation time does not change the diffusion length of the DDAN molecules from formula (3). Thus it is supposed that the branches can be formed firstly and become longer and longer with the increasing evaporation time. When the branch length L is longer than the diffusion distance λ, statistically speaking, molecules are no longer able to reach the branch top to form longer branches, and instead they form short branches at the side of long branches. Furthermore, with the increasing evaporation time, molecules should reach the substrate uninterruptedly and diffuse immediately so that molecules should hit each other more frequently to lose their kinetic energies quickly, leading to the formation of particles.

Figure 4 shows the AFM images of the patterns obtained at different substrate temperatures. At 25°C substrate temperature, there are dense particles all over the substrate with a diameter of about 600 nm (Fig. 4(a)). At substrate temperature 30°C, nearly 2 μm diameter particles aggregate together in small regions of the substrate (Fig. 4(b)). At substrate temperature 30°C, there are 25-μm-long branches formed and attached to small particles (Fig. 4(c)). At 40°C, much longer branches of about 30 μm are obtained and scarcely all the particles are attached to these branches (Fig. 4(d)). At higher substrate temperature, there are nearly no molecules stayed on the substrate. Thus, it can be concluded that the transformation of the desert into the forest patterns is due to the increase of the substrate temperature.

Low substrate temperature limits the surface diffusion of the adsorbates to produce an amorphous film.[34] In our case, the high kinetic energy at high substrate temperature reduces the diffusion activation energy E_d and the deposition rate R. Thus according to Eq. (3), the diffusion distance λ of the DDAN molecules should become longer when the substrate temperature is increased to reduce E_d and R. Therefore molecules should diffuse a long distance at high substrate temperature to form long branches. The

amount of the evaporated molecules can also change pattern formation. For example, more 0.01 g DDAN molecules is added into the quartz crucible while other experimental parameters are kept as the same as those of the sample shown in Fig. 3(a). Complete different results are observed. It can be seen that dense particles aggregate into clusters and a few of the central branches are distinguished from the clusters as shown in Fig. 5. This pattern is totally different from the long branches achieved with less amount of molecule deposition. More deposition of molecules brings in a greater amount of the beam to result in a greater deposition rate R. Thus molecules should hit each other much more frequently to limit their diffusion, leading to a small diffusion distance λ (Eq. (3)). Therefore, particles are formed through aggregation as opposed to the formation of branches at the low deposition rate.

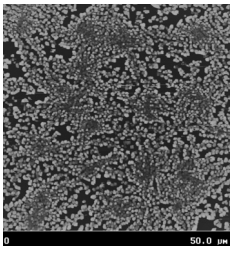

Fig. 5. AFM image of the organic patterns evaporated at 90°C for 1 min on SiO_2 substrate. The evaporation amount is 0.02 g, $P = 4.0 \times 10^{-6}$ Torr. The formation of the desert pattern is due to the high deposition rate which limits the diffusion distance.

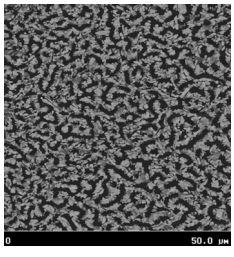

Fig. 6. AFM image of a net-like pattern on hexagonal lattice of mica (001) surface. The deposition lasts for 3 min at 90°C evaporation temperature, and the pressure is 5.0×10^{-6} Torr.

Different substrates were used to single out the effect of the substrate on the pattern formation. DDAN molecules were deposited on a mica substrate with the same experimental parameters as those in Fig. 3(b). Different patterns are obtained as shown in Fig. 6 with neither branches nor particles, but a net-like pattern with a stripe width of about 1.6 μm. Mica is a monoclinic crystal, and the surface facet of (001) is a hexagonal lattice.[35] Due to the fact that there is much stronger interaction between the mica surface and the DDAN molecules, the molecules are no longer able to diffuse freely except along a specific direction. Therefore net-like patterns are achieved on mica substrate rather than branches and particles on the amorphous SiO_2 substrate.

Fractal forest and desert patterns of DDAN molecules are controllably achieved on amorphous SiO_2 substrates. The evaporation temperature and time, substrate temperature, and the amount of the deposition are varied to explore the transition between these two patterns. A thermal kinetic formula is used to explain the transformation between the forest pattern and the desert pattern. We also find that these novel patterns cannot be formed on mica substrates, which is attributed to the strong interaction between mica and the DDAN molecules. These experimental results are helpful for designing different molecules which have similar structures as DDAN molecules.

References

[1] Forrest S R 1997 *Chem. Rev.* **97** 1793
[2] O'Neil M P, Niemczyk M P, Svec W A, Gosztola D, Gaines G L and Wasielewski M R 1992 *Science* **257** 63
[3] Mandelbrot B B 1982 *Fractal Geometry of Nature* (New York: Freeman)
[4] Li C R, Zhang X N and Cao Z X 2005 *Science* **309** 909
[5] Gao H J et al 2000 *Phys. Rev. Lett.* **84** 1780
[6] Shi D X, Wang Y L, Zhang H X, Jiang P, He S T, Pang S J and Gao H J 2000 *Appl. Phys. Lett.* **77** 3203
[7] Shi D X, Song Y L, Zhu D B and Gao H J 2001 *Adv. Mater.* **13** 1103
[8] Feng M et al 2005 *J. Am. Chem. Soc.* **127** 15338
[9] Gao H J, Canright G S, Pang S J et al 1998 *Fractals* **6** 337
[10] Sandler I M, Canright G S, Zhang Z Y et al 1998 *Phys. Rev.* A **245** 233
[11] Service R F 2001 *Science* **293** 1746
[12] Zhang Z Y and Lagally M G 1997 *Science* **276** 377
[13] Witten T A and Sander L M 1981 *Phys. Rev. Lett.* **47** 1400
[14] Brechignac C et al 2002 *Phys. Rev. Lett.* **88** 196103
[15] Wang M et al 1998 *Phys. Rev. Lett.* **80** 3089
[16] Wang Y L et al 2005 *Phys. Rev. Lett.* **94** 106101
[17] Gao L et al 2006 *Phys. Rev.* B **73** 075424
[18] Shi D X, Ji W, Lin X, He X B, Lian J C, Gao L et al 2006 *Phys. Rev. Lett.* **96** 226106
[19] Du S X, Gao H J and Seidel C 2006 *Phys. Rev. Lett.* **97** 156105
[20] Ravagnan L et al 2002 *Phys. Rev. Lett.* **89** 285506
[21] Liu B G, Wu J, Wang E G and Zhang Z Y 1999 *Phys. Rev. Lett.* **83** 1195
[22] Krause B et al 2002 *Phys. Rev.* B **66** 235404
[23] Gao H J, Xue Z Q, Wang K Z, Wu Q D and Pang S J 1996 *Appl. Phy. Lett.* **68** 2192
[24] Gao H J, Xue Z Q, Wu Q D and Pang S J 1995 *J. Vacuum Sci. Technol.* B **13** 1242
[25] Melby C R et al 1962 *J. Am. Chem. Soc.* **84** 3374
[26] Carroll R L and Gorman C B 2002 *Angew. Chem. Int. Ed.* **41** 4378
[27] Grabowski Z R, Rotkiewicz K and Rettig W 2003 *Chem. Rev.* **103** 3899
[28] Bosch P et al 2002 *J. Photochem. Photobiol. A: Chem.* **153** 135
[29] Bosch P et al 2000 *J. Photochem. Photobiol. A: Chem.* **133** 51
[30] Hakala K et al 2000 *Macromolecules* **33** 5954
[31] Wu H M, Song Y L, Du S X, Liu H W, Gao H J, Jiang L and Zhu D B 2003 *Adv. Meter.* **15** 1925
[32] Wen Y Q, Song Y L, Gao H J et al 2004 *Adv. Mater.* **16** 2018
[33] Jiang G Y, Feng M, Wen Y Q, Du S X, Gao H J et al 2005 *Adv. Mater.* **17** 2170
[34] Ruiz R et al 2004 *Chem. Mater.* **16** 4497
[35] Hartman H, Sposito G and Yang A 1990 *Clays and Clay Minerals* **38** 337